

Stability of free-convection flows of variable-viscosity fluids in vertical and inclined slots

By YEN-MING CHEN AND ARNE J. PEARLSTEIN

Department of Aerospace and Mechanical Engineering, University of Arizona,
Tucson, AZ 85721, USA

(Received 3 November 1987 and in revised form 5 July 1988)

The stability of the buoyancy-driven parallel shear flow of a variable-viscosity Newtonian fluid between vertical or inclined plates maintained at different temperatures is studied theoretically. The analysis is capable of dealing with arbitrary viscosity–temperature relations. Depending on the Prandtl number, angle of inclination, and form of the viscosity–temperature variation, the flow may become unstable with respect to two-dimensional longitudinal or transverse disturbances. Outstanding questions arising in previous investigations of the stability of parallel free-convection flows of constant-viscosity fluids in inclined slots and of variable-viscosity fluids in vertical slots are discussed. We find that, in a variable-viscosity fluid, non-monotonic dependence of the critical Rayleigh number on the inclination angle can occur at significantly higher Prandtl numbers than is possible in the constant-viscosity case. Results are also presented for the stability of the free-convection flow of several glycerol–water solutions in an inclined slot.

1. Introduction

Free convection in vertical and inclined slots and its dependence on geometry, Prandtl number (Pr), and Rayleigh number are of practical importance in a number of heat transfer, materials processing, and other applications. The stability of the various flow regimes and the transitions between them have important consequences for the relevant technological processes. For current reviews, the reader is referred to Catton (1978), Ostrach (1982), Raithby & Hollands (1985), and Hoogendoorn (1986).

Recently, Goldstein & Wang (1984) have pointed out the importance of temperature-dependent thermophysical properties in determining the onset of instability in these flows. The object of the present work is to investigate the stability of parallel free-convection flows of variable-viscosity fluids in vertical and inclined slots, the importance of which derives from the fact that the temperature dependence of the viscosity is the most important non-Boussinesq effect in many applications (Carey & Mollendorf 1978).

The stability of the parallel free-convection flow of a constant-viscosity fluid in a vertical slot was first considered by Gershuni (1953) and Batchelor (1954). Several others (Rudakov 1966, 1967; Vest & Arpaci 1969; Gill & Kirkham 1970; Birikh *et al.* 1972; Korpela, Gözüüm & Baxi 1973; Ruth 1979) have subsequently studied the problem, both experimentally and theoretically. In the vertical case, there is a preferred orientation for the disturbance planform at onset (and ultimately, of the secondary flow), and the Prandtl number strongly affects the onset of instability, which is steady at small Pr and oscillatory at larger Pr .

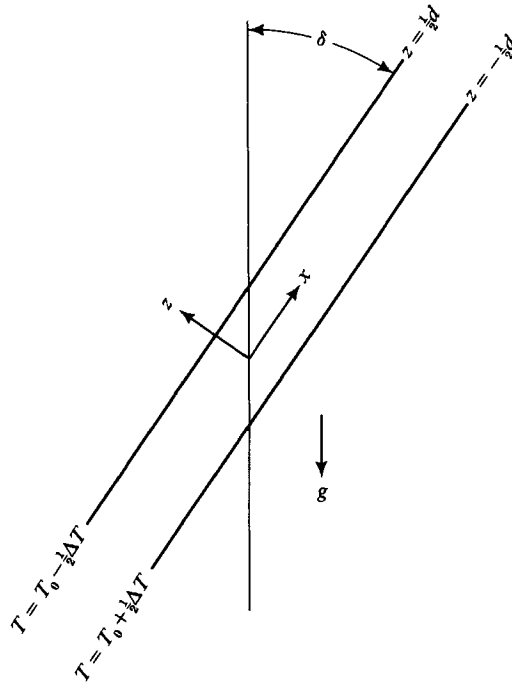


FIGURE 1. Definition sketch and coordinate system for the inclined slot. The spanwise coordinate y is perpendicular to the page.

Work on the stability of this free-convection flow has been extended in several directions. One extension has been to study non-Boussinesq effects and, in particular, the dependence of the viscosity on temperature (Seki, Fukusako & Inaba 1978; Chen & Thangam 1985; Thangam & Chen 1986; Smith 1988). Another extension has been to consider fluid-filled slots arbitrarily inclined with respect to the vertical (Gershuni 1955; Birikh *et al.* 1968; Kurzweg 1970; Hart 1971; Hollands & Konicek 1973; Korpela 1974; Ruth 1980; Ruth, Hollands & Raithby 1980; Goldstein & Wang 1984). In a theoretical study of the stability of constant-viscosity free-convection flows in an inclined box, Hart (1971) found the extremal Rayleigh number for the transverse mode to be a multivalued function of the inclination angle δ , measured from the vertical (figure 1), in a small range of δ near 66° at $Pr = 6.7$ (corresponding to water). For inclined layers with $Pr = 6.7$ heated from below, the onset of instability occurs via the transverse mode when $\delta \leq 2^\circ$. The range of δ for which the transverse mode is critical is larger ($\delta \leq 19^\circ$) for $Pr = 0.71$ (air). (Transverse and longitudinal modes correspond to disturbances with no y -dependence and x -dependence, respectively. See figure 1 for the coordinate system.)

Previous work on the stability of free-convection flows of constant-viscosity fluids in vertical and inclined slots and of variable-viscosity fluids in vertical slots has raised a number of unresolved questions. In the constant-viscosity case, points on which previous workers disagree or the results are otherwise in doubt include:

(1) *the disagreement among theoretical predictions of the transition Prandtl number, Pr^* at which the preferred mode of instability of the free-convection flow in a vertical slot changes from steady to oscillatory.* Reported values include 12.0–12.5 (Brenier, Roux

& Bontoux 1986), 12.7 (Korpela *et al.* 1973), 11.4† (Gershuni & Zhukhovskii 1976) and 25 (Thangam & Chen 1986);

(2) *the theoretical finding by Ruth (1980) of a 'virtual discontinuity' in the dependence on Pr of the Rayleigh number for the transverse mode for an inclined slot.* We shall show that this is closely related to the closed disconnected neutral curves (CDNC) discovered by Hart (1971). We shall also investigate whether there are conditions for which flows corresponding to Rayleigh numbers lying *above* the CDNC are in fact stable with respect to all two-dimensional (longitudinal and transverse) disturbances.

For free-convection flow of a variable-viscosity fluid in a vertical slot, questions arise regarding:

(3) *how the functional form of the viscosity-temperature relation $\mu(T)$ affects the stability.* This question is also of interest in relation to the experimental work of Seki *et al.* (1978) and Chen & Thangam (1985) using transformer oil and aqueous glycerol solutions (see (4) below) and in connection with the assertion of Thangam & Chen (1986) that the stability criteria are independent of $\mu(T)$ for $Pr \leq 100$.

(4) *the systematic discrepancies between the experimental and theoretical results of Chen & Thangam (1985) for the onset of instability.* One possible explanation relates to their use of an exponential approximation $\mu_e(T) = S \exp(-sT)$ to the actual $\mu(T)$.

The foregoing questions and the remarks of Goldstein & Wang (1984) provided the original motivation for the present work. We use linear stability theory to address these questions and related issues concerning the onset of instability in free-convection flows of variable-viscosity fluids, including aqueous glycerol solutions, in vertical and inclined slots. To the best of our knowledge, the stability of free-convection flows of variable-viscosity fluids in inclined slots has not been previously investigated.

The problem formulation and basic state are presented in §2. The linear stability analysis is described in §3. The physical properties of aqueous glycerol solutions are discussed in §4. Points (1)–(3) above and related issues are addressed in §5, followed by a discussion of (4) in §6.

2. Formulation and the basic state

We consider the stability of two-dimensional free-convection flow between two perfectly conducting plates separated by a gap d and maintained at constant temperatures differing by ΔT , as shown in figure 1. The plates are inclined at an angle δ to the vertical. We choose a Cartesian coordinate system, where the x - and z -axes are parallel and normal to the plates, respectively. The origin of the coordinate system is located in the midplane of the layer. We assume that all physical properties of the fluid are constant except the dynamic viscosity μ , which is an arbitrary function of temperature, and the density ρ , which is taken to be constant except in the body-force term of the momentum equation, where it is allowed to depend linearly on temperature, according to

$$\rho(T) = \rho_0[1 - \alpha(T - T_0)],$$

† Unfortunately, the expansion functions used in the Galerkin procedure of Gershuni & Zhukhovitskii are not part of a complete set, as previously shown by Gallagher (1969).

where ρ_0 is the density at the reference temperature T_0 and α is the thermal expansivity. The subscript 0 denotes midplane values of variable quantities.

The governing equations are taken to be the spanwise component of the vorticity transport equation (because the linear stability analysis can be restricted to two-dimensional disturbances as discussed in §3) and the energy equation with the viscous-dissipation term neglected. We use d as the characteristic length, ΔT as the characteristic temperature, and the thermal diffusion time d^2/κ [where $\kappa = k/(\rho_0 c_p)$] is the thermal diffusivity, k is the thermal conductivity, and c_p is the specific heat] as the characteristic time. The non-dimensional equations are

$$\frac{1}{Pr} \frac{D\omega}{Dt} = f \nabla^2 \omega - Ra \left(\sin \delta \frac{\partial \theta}{\partial x} - \cos \delta \frac{\partial \theta}{\partial z} \right) + 2 \frac{\partial f}{\partial z} \nabla^2 u - 2 \frac{\partial f}{\partial x} \nabla^2 w + \left(\frac{\partial^2 f}{\partial z^2} - \frac{\partial^2 f}{\partial x^2} \right) \left(\frac{\partial u}{\partial z} + \frac{\partial w}{\partial x} \right) + 4 \frac{\partial^2 f}{\partial x \partial z} \frac{\partial u}{\partial x}, \quad (2.1)$$

$$\frac{D\theta}{Dt} = \nabla^2 \theta, \quad (2.2)$$

where $\nabla^2 = \partial^2/\partial x^2 + \partial^2/\partial z^2$, $\omega = \partial u/\partial z - \partial w/\partial x$ is the spanwise vorticity component, $Ra = (\rho_0 \alpha g \Delta T d^3)/(\mu_0 \kappa)$ is the Rayleigh number, $Pr = \mu_0/(\rho_0 \kappa)$ is the Prandtl number, $\theta = (T - T_0)/\Delta T$ is the dimensionless temperature, and $f(\theta) = \mu(T_0 + \theta \Delta T)/\mu_0$ is a dimensionless function. The boundary conditions are

$$u = w = 0 \quad \text{at } z = \pm \frac{1}{2}, \quad (2.3)$$

$$\theta = \mp \frac{1}{2} \quad \text{at } z = \pm \frac{1}{2}. \quad (2.4)$$

These equations admit a basic solution which consists of a parallel flow in the x -direction, $\mathbf{u} = (u_b, 0, 0)$ with a temperature distribution $\theta_b(z) = -z$. The velocity profile satisfies

$$\frac{d^2}{dz^2} \left[f(\theta_b) \frac{du_b}{dz} \right] = Ra \cos \delta. \quad (2.5)$$

For a given viscosity-temperature relation $f(\theta)$, (2.5) can be integrated to obtain u_b , subject to the no-slip boundary conditions (2.3) and the global continuity constraint

$$\int_{-\frac{1}{2}}^{\frac{1}{2}} u_b dz = 0.$$

3. Linear stability analysis

The Squire *transformation* developed by Gershuni & Zhukhovitskii (1969) for a constant-viscosity fluid in an inclined slot can be easily extended to the variable-viscosity case. However, as pointed out by Hart (1971), even in the constant-viscosity case there is no Squire's *theorem*, in the sense of Gage & Reid (1968). That is, two-dimensional disturbances are not always more unstable than three-dimensional ones with the same total wavenumber. Thus, as will be discussed in §5, stability of the basic state with respect to small two-dimensional transverse waves does not guarantee stability with respect to infinitesimal oblique disturbances. This is because for the transverse mode there may be a CDNC lying below the minimum of the 'primary' neutral curve, as described by Pearlstein (1981) in another context. Thus, in addition to the semi-infinite range of Ra lying below the globally minimum

value of Ra , there may also be a finite range of Ra lying between the primary neutral curve and the CDNC, in which the flow is linearly stable with respect to arbitrary transverse disturbances, but is linearly unstable with respect to oblique disturbances.

Nevertheless, the stability analysis can be restricted to two-dimensional disturbances (longitudinal rolls or transverse waves) because the CDNC is found only for combinations of Pr and δ for which the *longitudinal mode* becomes unstable at a Rayleigh number lying below the minimum of the CDNC. Gershuni & Zhukhovitskii (1969) and Kurzweg (1970) showed that the criterion for onset of the longitudinal mode in an inclined slot is easily obtained from the Rayleigh number for onset of convection in a horizontal layer. Their result carries over directly to the variable-viscosity case. For fixed δ , the Rayleigh number at which the flow first becomes unstable with respect to longitudinal rolls is given by

$$Ra_{lon}(\delta) = Ra_{crit}(90^\circ)/\sin \delta. \tag{3.1}$$

Here, $Ra_{crit}(90^\circ)$ is the critical Rayleigh number at which convection sets in for a horizontal layer ($\delta = 90^\circ$) with the same $f(\theta)$. In the inclined case, the critical Rayleigh number $Ra_{crit}(\delta)$ will be the smaller of $Ra_{lon}(\delta)$ and $Ra_{tra}(\delta)$, where $Ra_{tra}(\delta)$ is the smallest Ra at which the flow is linearly unstable with respect to transverse waves. In the cases examined in §5, the CDNC occurs only for combinations of Pr and δ for which longitudinal rolls are unstable at a smaller Ra , so that the flow is stable only in a semi-infinite range of Ra . Thus, only one value of Ra , namely Ra_{crit} , will be required to specify the stability criteria, unlike the other cases in which CDNCs have been found (Pearlstein 1981; Pearlstein, Harris & Terrones 1988). The remainder of the analysis will therefore be devoted to the determination of Ra_{tra} .

Decomposing the velocity and temperature into

$$[u, w, \theta] = [u_b + u', 0 + w', \theta_b + \theta'], \tag{3.2}$$

where the prime denotes the disturbance quantities, we characterize u' by a stream function ψ'

$$u' = \frac{\partial \psi'}{\partial z}, \quad w' = -\frac{\partial \psi'}{\partial x} \tag{3.3 a, b}$$

and consider disturbances of the form

$$[\psi', \theta'] = [\hat{\phi}, \hat{\theta}] \exp(i\beta x + \sigma t), \tag{3.4 a, b}$$

where β is the (real) wavenumber in the x -direction and σ is the temporal growth rate, which in general is complex. Substituting (3.2)–(3.4) into (2.1) and (2.2) and retaining only first-order terms, the linear disturbance equations can be written as

$$\begin{aligned} f(\theta_b) [(D^2 - \beta^2)^2 \hat{\phi}] - \frac{i\beta}{Pr} [u_b(D^2 - \beta^2) \hat{\phi} - (D^2 u_b) \hat{\phi}] \\ - 2[D_\theta f(\theta_b)] (D^3 - \beta^2 D) \hat{\phi} + [D_\theta^2 f(\theta_b)] (D^2 + \beta^2) \hat{\phi} \\ + \{Ra \cos \delta + 2[D_\theta f(\theta_b)] D^2 u_b - 2[D_\theta^2 f(\theta_b)] D u_b\} D \hat{\theta} \\ - \{i\beta Ra \sin \delta - [D_\theta f(\theta_b)] D^3 u_b + 2[D_\theta^2 f(\theta_b)] D^2 u_b \\ - [D_\theta^3 f(\theta_b)] D u_b - [D_\theta f(\theta_b)] D u_b (D^2 + \beta^2)\} \hat{\theta} - \frac{\sigma}{Pr} (D^2 - \beta^2) \hat{\phi} = 0, \end{aligned} \tag{3.5}$$

$$(D^2 - \beta^2) \hat{\theta} - i\beta \hat{\phi} - i\beta u_b \hat{\theta} - \sigma \hat{\theta} = 0, \tag{3.6}$$

where $D = d/dz$ and $D_\theta = d/d\theta$.

The boundary conditions are

$$\hat{\phi} = \frac{d\hat{\phi}}{dz} = \hat{\theta} = 0 \quad \text{at} \quad z = \pm \frac{1}{2}. \quad (3.7a-c)$$

We note that, by setting $\delta = 0$, (3.5) and (3.6) reduce to the linear disturbance equations for the vertical-slot case studied by Thangam & Chen (1986).

The disturbance quantities $\hat{\phi}$ and $\hat{\theta}$ are expanded in terms of complete sets of trial functions

$$\hat{\phi}(z) = \sum_{n=1}^{\infty} a_n \phi_n(z) \quad (3.8)$$

and

$$\hat{\theta}(z) = \sum_{n=1}^{\infty} b_n \theta_n(z) \quad (3.9)$$

that satisfy the homogeneous boundary conditions (3.7), where the functions

$$\phi_n(z) = \begin{cases} \frac{\cosh(\alpha_n z)}{\cosh(\alpha_n/2)} \frac{\cos(\alpha_n z)}{\cos(\alpha_n/2)} & (n \text{ odd}) \\ \frac{\sinh(\alpha_n z)}{\sinh(\alpha_n/2)} \frac{\sin(\alpha_n z)}{\sin(\alpha_n/2)} & (n \text{ even}) \end{cases}$$

are described by Chandrasekhar (1961), the constants α_n are zeros of

$$\begin{aligned} \tanh(\alpha_n/2) + \tan(\alpha_n/2) &= 0 & (n \text{ odd}), \\ \coth(\alpha_n/2) - \cot(\alpha_n/2) &= 0 & (n \text{ even}) \end{aligned}$$

and the functions θ_n are given by

$$\theta_n(z) = \begin{cases} \cos(n\pi z) & (n \text{ odd}) \\ \sin(n\pi z) & (n \text{ even}). \end{cases}$$

The expansions (3.8) and (3.9) are substituted into the disturbance equations (3.5) and (3.6), and a Galerkin method, in which the residuals are required to be orthogonal to the trial functions, is used to obtain an infinite number of linear homogeneous algebraic equations for a_n and b_n (Finlayson 1972). We then seek the value of Ra at which infinitesimally small transverse disturbances of all wavenumbers decay, except for those at one (or possibly several) critical wavenumber(s), which are neutral (i.e. disturbances neither grow nor decay). In order to obtain a finite number of linear homogeneous algebraic equations, we truncate expansions (3.8) and (3.9) at M and N terms, respectively, multiply (3.5) by ϕ_j ($1 \leq j \leq M$) and (3.6) by θ_j ($1 \leq j \leq N$), and integrate from $z = -\frac{1}{2}$ to $\frac{1}{2}$. The integrals are performed numerically (Gaussian quadrature), thus allowing for $f(\theta)$ to depend arbitrarily on temperature. We are left with a matrix eigenvalue problem of the form

$$(\mathbf{A} + \sigma \mathbf{B}) \mathbf{X} = \mathbf{0},$$

where \mathbf{A} and \mathbf{B} are known matrices and \mathbf{X} is a vector containing the unknown coefficients a_n and b_n .

This generalized matrix eigenvalue problem can be solved by standard numerical techniques (see, for example, Garbow *et al.* 1977). The eigenvalues σ depend on the inclination angle δ , the Rayleigh number Ra , the Prandtl number Pr , the wavenumber β and the viscosity-temperature relation $f(\theta)$. For a given $f(\theta)$ and set of parameters δ , Ra , Pr , β , the number of eigenvalues is equal to the sum of the

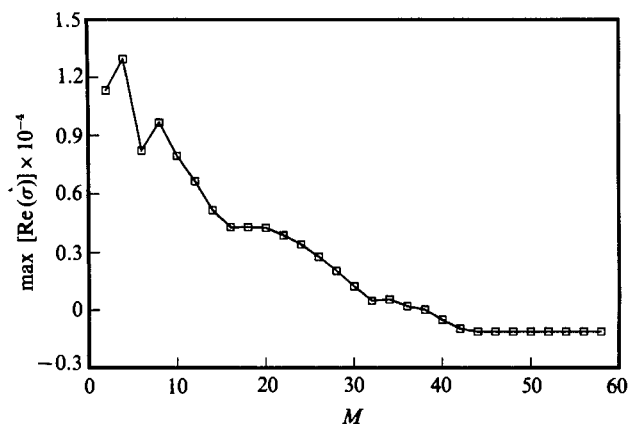


FIGURE 2. Temporal growth rate as a function of the truncation parameter M . $f(\theta) = \exp(-\theta)$, $Ra = 2.6 \times 10^6$, $Pr = 100$, $\beta = 4.25$, $\delta = 0^\circ$.

numbers (M and N) of trial functions used in (3.8) and (3.9), respectively. We note that the basic free-convection flow [which depends on Ra , $f(\theta)$ and δ] is unstable if for any β there is a value of σ lying in the right half-plane. We seek the value Ra_{tra} for which transverse disturbances decay for all β , except at one or more wavenumbers for which some eigenvalues lie on the imaginary axis with no σ in the right half-plane.

We take the truncation parameters M and N to be equal. For each combination of Ra and β , we increase M and N by two each until both the real and imaginary parts of the σ having the largest growth rate differ by less than 1% for three successive even values of M . The stringency of this criterion is justified by inspection of figure 2, which shows the growth rate (real part of the least stable or most unstable σ) as a function of the truncation parameter M (or N) for a wavenumber near the vertical asymptote of the neutral curve, with Ra near the neutral curve. In this extreme case, we have carried the calculation to 58 terms to demonstrate that satisfaction of the 1% convergence criterion (at $M = 48$) does indeed correspond to a converged solution. Notice that the 1% convergence criterion is not met until 48 terms are used in expansions (3.8) and (3.9). False convergence (of a type less readily detectable than that reported by Denn 1975) would have been mistakenly accepted at 20 terms had we set the criterion to be, say, 2%. We would have erroneously concluded that the basic flow with $Ra = 2.6 \times 10^6$, $\delta = 0$, and $f(\theta) = \exp(-\theta)$ was unstable for $Pr = 100$ with respect to transverse disturbances with $\beta = 4.25$, whereas in fact it is not. A convergence criterion more stringent than 1% would increase the cost significantly; we feel that the present choice is a good one. For points near Ra_{tra} and the corresponding β , fewer than 30 terms are normally required to meet the 1% convergence criterion. All calculations were performed with 64-bit precision arithmetic.

For a fixed β , the marginally stable point(s) on the neutral curve is (are) obtained by iteratively adjusting Ra (using bisection or the secant rule to drive the growth rate to zero) until two successive values of Ra differ by less than 0.1%. We refer to this as a vertical iteration.

To locate an extremal point on the neutral curve, we fix Ra and determine the value of β (from among ten equidistantly spaced values, typically in the range $0.5 \leq \beta \leq 5.0$) for which the growth rate is largest. We call this a horizontal

(wavenumber) traverse. If none of these values of β yields a positive growth rate, then Ra is doubled, and the horizontal traverse is repeated until an unstable Ra is located. Because the bisection or secant rule used in the vertical iteration is a two-point scheme, we need a second value of Ra for which the growth rate is known. This is obtained by halving Ra (possibly more than once) until a stable value of Ra (at the same β) is found. The vertical iteration then yields a point on the neutral curve. The extremal point is finally located by an alternating sequence of horizontal traverses and vertical iterations, with the horizontal traverses covering ten points bounded by the values of β from the previous horizontal traverse which were adjacent to the β used in the immediately preceding vertical iteration. This process is continued until the neutral values of Ra obtained on successive vertical iterations differ by less than 0.1%.

Since there may be more than one local minimum on a neutral curve or there may even be more than one neutral curve, it is necessary to ensure that the extremal Rayleigh number obtained is the critical one. To this end we perform a horizontal traverse at the first extremal Rayleigh number obtained. Wavenumbers greater and less than the extremal β are checked to see if an unstable region exists to the left or right of the known extremum. If an unstable region is detected, the procedure described above is repeated to obtain the minimum extremal Rayleigh number Ra_{tra} .

When the transverse wave instability sets in as a stationary disturbance, points on the neutral curve correspond to $\sigma = 0$. The generalized eigenvalue problem then becomes

$$(\mathbf{P} + Ra \mathbf{Q}) \mathbf{Y} = \mathbf{0},$$

where Ra is the eigenvalue. This requires much less computation since one need not iterate on Ra in order to determine points on the Ra - β neutral curve.

As a check on our numerical scheme, the calculation of Stengel, Oliver & Booker (1982) for a variable-viscosity fluid in a horizontal slot was repeated by setting $\delta = 90^\circ$. We used the exponential form of $\mu(T)$, and found the variation of Ra_{tra} with viscosity contrast (the ratio of viscosity at the cold wall to that at the hot wall) to be the same as that of the Ra_{crit} obtained by Stengel *et al.* We also calculated Ra_{tra} for a constant-viscosity fluid in an inclined slot (of infinite spanwise and streamwise extent) and obtained excellent agreement with Hart's (1971) numerical results for $Pr = 6.7$ (water) in a finite box of aspect ratio 10^4 . The values of Ra_{tra} we obtained for constant-viscosity free-convection flow in an infinite slot at $\delta = 66^\circ$ and 78° differ from those of Hart by less than 2%, which is the accuracy that Hart ascribed to his calculation when 14 terms were retained in the expansions.

4. Properties of aqueous glycerol solutions

In our study of the stability of free-convection flows of variable-viscosity fluids, we shall devote considerable attention to aqueous glycerol solutions, since they have been used in several experimental studies (Seki *et al.* 1978; Chen & Thangam 1985; Thangam & Chen 1986). In most applications, the variation of viscosity with temperature is the most important non-Boussinesq effect. Moreover, the viscosities of these highly associated liquids deviate considerably from the commonly used exponential and Arrhenius [$\mu(T) = R \exp(r/T)$] approximations (Litovitz 1952; Chen & Pearlstein 1987). For a 90% glycerol solution and $0 \leq T \leq 100^\circ \text{C}$, the maximum errors incurred by use of the exponential and Arrhenius approximations are 47.25% and 29.47%, respectively.

For a nominally motionless horizontal layer, we have found (Chen & Pearlstein 1988) that the exponential form used to approximate the actual $\mu(T)$ data can be responsible for errors considerably greater than the uncertainty in careful measurements of ΔT_{crit} . For concentrated aqueous glycerol solutions with $T_0 = 25^\circ\text{C}$ and $\Delta T = 20^\circ\text{C}$, the error is on the order of 3%, while for $T_0 = 50^\circ\text{C}$ and $\Delta T = 100^\circ\text{C}$, the error is on the order of 15%.

When the basic state is not motionless, we might expect the form of $\mu(T)$ to be more important, because the onset of secondary flow may now occur through a hydrodynamic mechanism. Also, the linear disturbance equations contain a third derivative of μ with respect to T , so that the stability of the base flow might be expected to depend more sensitively on the exact form of $\mu(T)$.

Given that the exponential and Arrhenius forms poorly approximate $\mu(T)$ for aqueous glycerol solutions, and the potential sensitivity of the stability analysis to small errors in $\mu(T)$, we have developed a four-parameter fit of the form (Chen & Pearlstein 1987)

$$\mu(T) = H \exp(E/T^3 + FT + G/T),$$

where T is the absolute temperature. This is based on the Litovitz (1952)

$$\mu(T) = V \exp(v/T^3),$$

Arrhenius, and exponential forms, where E , F , G , and H are parameters (depending on solution composition) determined by least-squares fitting of the data of Segur & Oberstar (1951). It is clear that Ra_{tra} depends on both ΔT and T_0 . We take $T_0 = 20^\circ\text{C}$ for the glycerol-water solutions considered.

The specific heats c_p of aqueous glycerol solutions are obtained from the linear relation $c_p(\gamma) = \gamma c_{p,g} + (1-\gamma)c_{p,w}$ proposed by Segur (1953), where γ is the mass fraction of glycerol, and $c_{p,g}$ and $c_{p,w}$ are the specific heats of pure glycerol and water respectively. The former is calculated from the formula given in Touloukian & Makita (1970) while $c_{p,w}$ is taken from Weast, Astle & Beyer (1986). The computed values of $c_p(\gamma)$ agree well with the experimental data of DiPaola & Belleau (1975) for aqueous glycerol solutions. They also agree well with the fitted data of Vedhanayagam, Lienhard & Eichhorn (1979) after mass fraction in that paper is corrected to mole fraction (private communications, J. H. Lienhard IV 1986, M. Vedhanayagam 1986). The thermal conductivity data are taken from Segur (1953).

5. Results and discussion

In the following, we present and discuss results bearing on the issues raised in §1. The disagreement in previous calculations of Pr^{tr} for free-convection flow of a constant-viscosity fluid in a vertical slot (point 1) is addressed in §5.1. In §5.2, point (2) is discussed in terms of the multivalued $Ra_{\text{tra}}-\delta$ curve for a constant-viscosity fluid in an inclined slot, and an explanation regarding the 'virtual discontinuity' in Ra_{tra} reported by Ruth (1980) is given. We also elucidate the sequence by which the number of neutral curves changes from one when $\delta = 0$ to infinity when $\delta = 90^\circ$. The various issues raised in point (3) of §1 are discussed in §5.3, where we also investigate the onset of secondary motion in a vertical slot occupied by a glycerol-water solution for which $\mu(T)$ cannot be accurately correlated by the exponential or Arrhenius forms. Finally, results for the stability of free-convection flows of variable-viscosity fluids in inclined slots are presented in §5.4.

5.1. Constant-viscosity fluid in a vertical slot

For free-convection flow of a constant-viscosity fluid in a vertical slot, the onset of instability may occur through either monotonically growing or oscillatory disturbances (Thangam & Chen 1986; Bergholz 1978). The two mechanisms have been described by Thangam & Chen, and can be briefly summarized as follows. The steady (i.e. monotonic) mode predicted at low Pr corresponds to onset via an instability of the parallel free-convection shear flow. Buoyancy is important only in setting up the basic state, and is not involved in the instability mechanism. At higher Pr , the oscillatory instability which they predicted and experimentally observed involves the buoyancy force in a more essential way.

The transition from the monotonically growing mode to the oscillatory mode has been studied by a number of authors. We find $12.4 < Pr^{tr} < 12.5$, in excellent agreement with the value of 12.7 reported by Korpela *et al.* (1973), and the range $12.0 < Pr^{tr} < 12.5$ obtained by Brenier *et al.* (1986). This value agrees less well with the values of 11.4 and 25 reported by Gershuni & Zhukhovitskii (1976) and Thangam & Chen (1986), respectively. The slight difference between our result and that of Korpela *et al.* (1973) may be attributed to our use of a fine wavenumber traverse in which the wavenumber range is iteratively subdivided down to an increment of 0.001.

Figures 3(a)–3(c) show the neutral curves at Prandtl numbers 12.5, 20, and 100, respectively. In figure 3(a, b) the neutral curve that lies on the larger wavenumber side corresponds to steady onset while the one to the left corresponds to oscillatory onset. At $Pr = 12.5$, the extrema of both neutral curves occur at virtually the same Grashof number $Gr_c = Ra/Pr$. As Pr increases, the oscillatory neutral curve grows in size while the steady neutral curve remains almost unchanged, as shown in figure 3(b). For the steady neutral curve, the insensitivity of Gr to Pr is to be expected since Gr is equivalent to the Reynolds number (Re) in the isothermal parallel shear flow problem, where the critical Re is independent of Pr . Figure 3(c) shows that, above a certain Pr , the two neutral curves intersect. The intersection is not a bifurcation point since the wave speed, $\text{Im}(\sigma)/\beta$, on the oscillatory neutral curve does not vanish there. In addition to quantitative differences, the neutral curves of Thangam & Chen (1986) differ topologically from ours (compare our figure 3b and their figure 4 at $Pr = 20$). Also, when our steady and oscillatory neutral curves are connected, the intersection is at a cusp (figure 3c), rather than through a smooth connection near the minima. For some Pr , our neutral curves appear to be disconnected (figure 3a, b). We note that the steady and oscillatory neutral curves reported for various Pr by Birikh *et al.* (1972), Bergholz (1978), and Shaaban & Özisik (1983) are qualitatively similar to ours, although the trial functions used by Birikh *et al.* do not form a complete set, the basic state considered by Bergholz includes a streamwise temperature gradient, and the equation of state used by Shaaban & Özisik includes a density maximum.

5.2. Constant-viscosity fluid in an inclined slot

Unlike those in vertical slots, parallel free-convection flows in inclined slots can become unstable via either longitudinal or transverse disturbances. For an inclined layer heated from above, the free-convection flow can still be unstable with respect to transverse disturbances, although it is stable with respect to longitudinal disturbances since the buoyancy force in this case is stabilizing. When studying the stability of free-convection flows in an inclined slot heated from above, there are two ways of presenting the results, as discussed by Hart (1971). The inclination angle δ

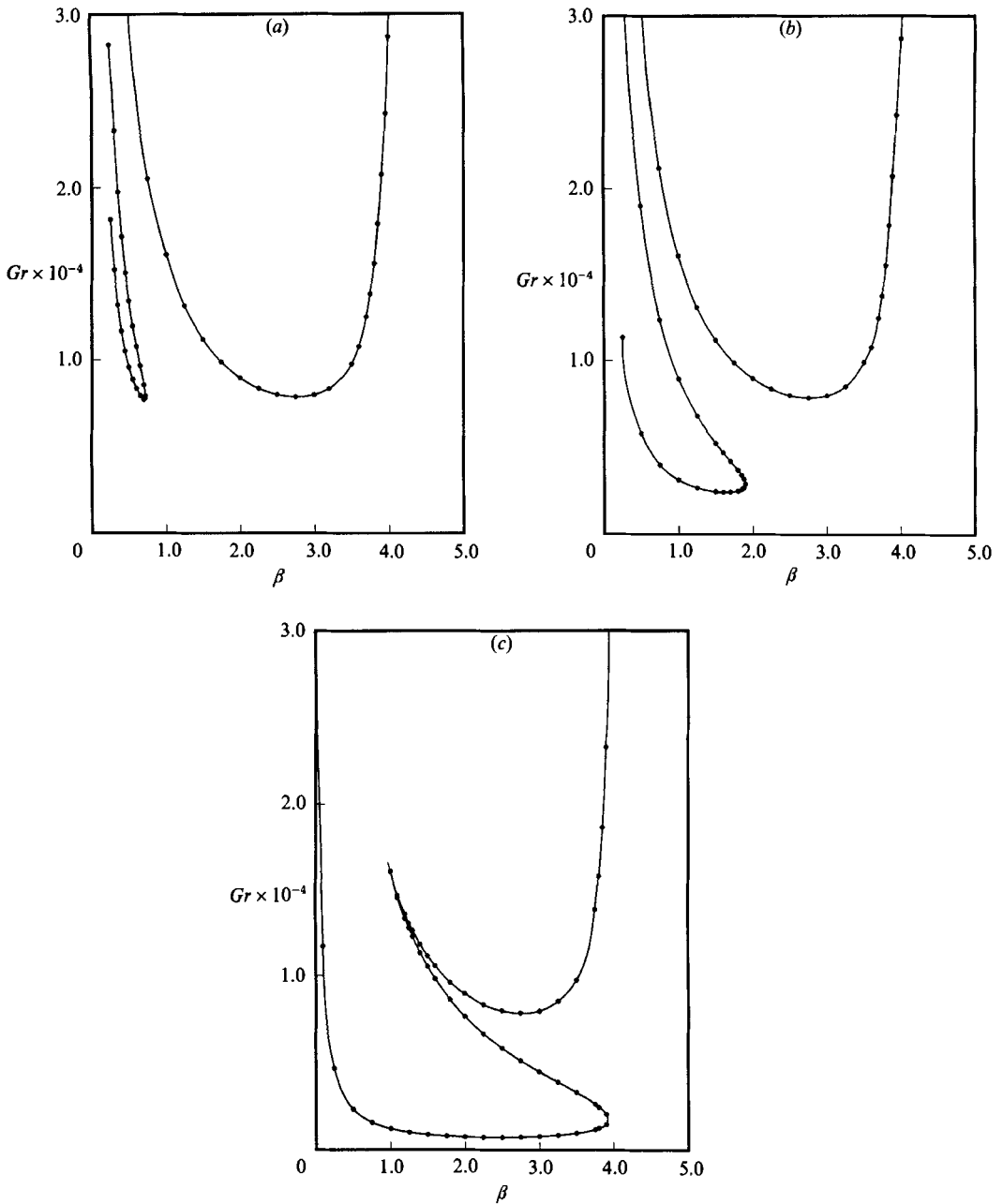


FIGURE 3. Neutral curves for a constant-viscosity fluid in a vertical slot. (● on neutral curve denotes a computed (β, Ra) pair.) (a) $Pr = 12.5$, (b) 20.0 , (c) 100.0 . Note that the neutral curves are disconnected for small Pr .

and temperature difference ΔT can be chosen as positive and negative, or negative and positive, respectively. The former yields negative values of Ra , corresponding to heating from above. We present results for $Pr = 6.7$ (water) in an inclined slot in this way in order to illustrate that there is another (disconnected) neutral curve on the opposite side of the Rayleigh-number axis, as shown in figure 4. The rest of our results will be presented in terms of positive ΔT .

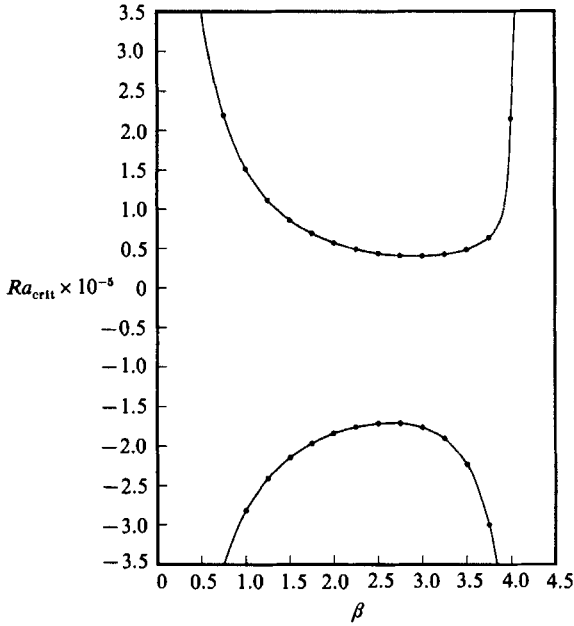


FIGURE 4. Neutral curves for a constant-viscosity fluid at $\delta = 30^\circ$, $Pr = 6.7$. Here, we have allowed ΔT (and hence Ra) to assume positive and negative values, while keeping the angle of inclination δ positive.

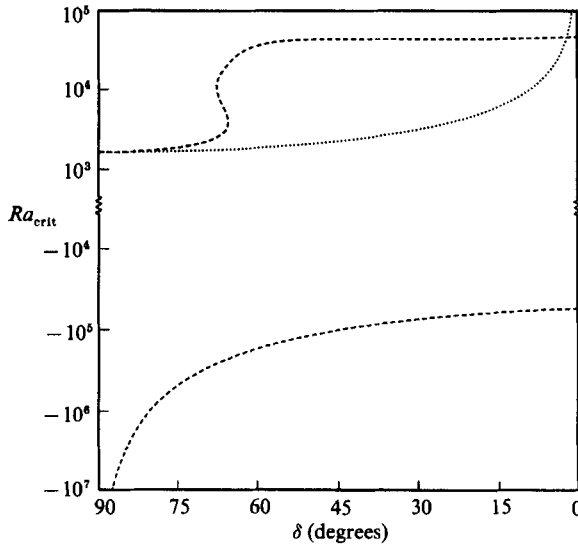


FIGURE 5. Stability boundary for a constant-viscosity fluid with $Pr = 6.7$ in an inclined slot. The flow is stable in the region between the longitudinal mode and the lower transverse mode, and for $0 \leq \delta \leq 2^\circ$, between the two transverse modes. \cdots , longitudinal mode; $---$, transverse mode.

Figure 5 shows the stability boundary for $Pr = 6.7$, for which results have been presented for positive ΔT over $-90^\circ \leq \delta \leq 90^\circ$ by Hart (1971). The S-shaped character of the upper branch of the transverse mode near $\delta = 66^\circ$ found by Hart deserves some additional comment. For $\delta \leq 65^\circ$ with ΔT positive, there is a single unimodal neutral curve, which assumes a minimum value at $\beta_{crit} \approx 3.1$. This neutral

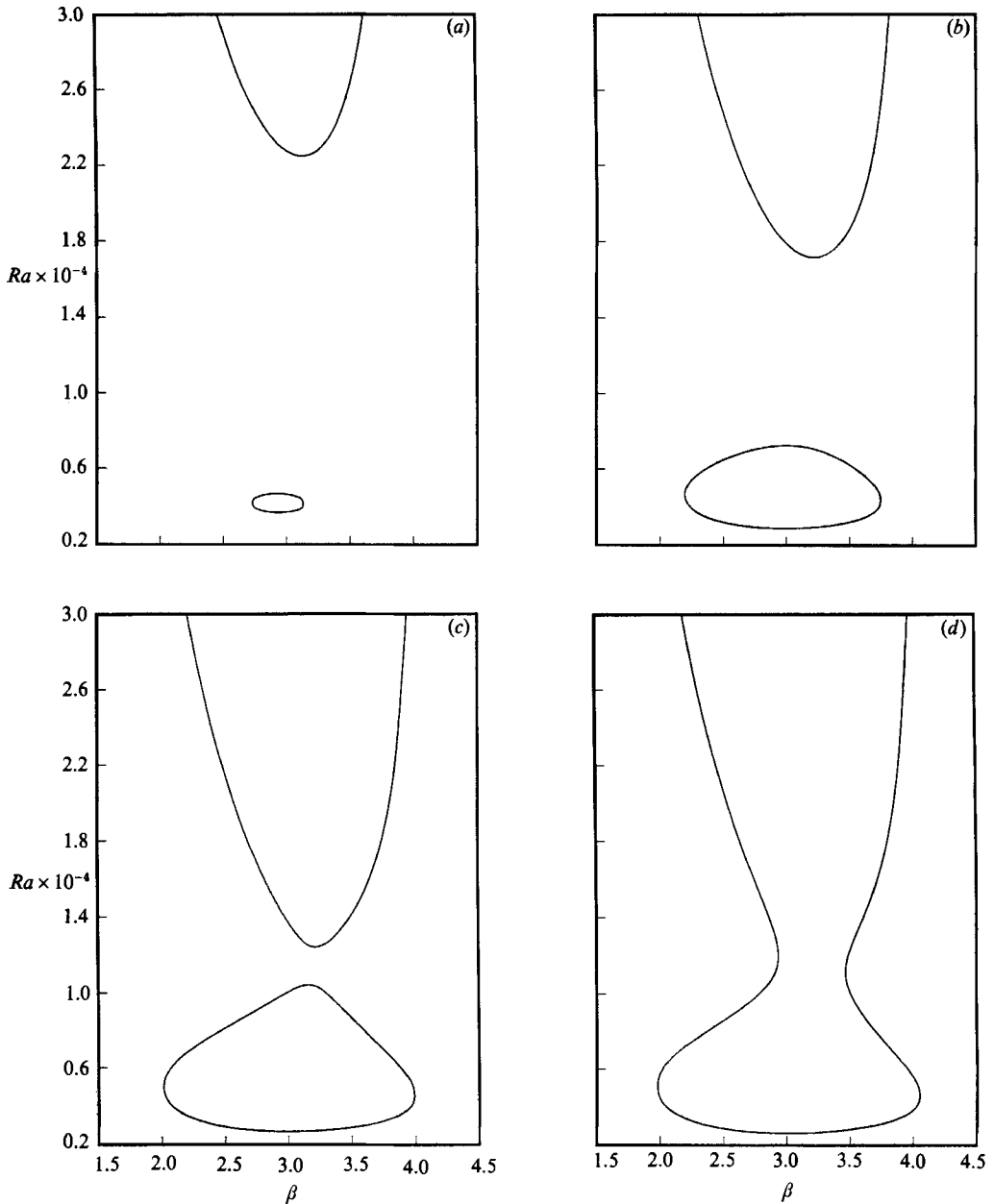


FIGURE 6. Neutral curve(s) for a constant-viscosity fluid with $Pr = 6.7$ at various δ . Note that the neutral curve separates into two disconnected neutral curves as δ decreases below 68° . The CDNC vanishes at a point for $\delta \approx 65.7^\circ$. (a) $\delta = 65.8^\circ$, (b) 67.0° , (c) 67.8° , (d) 68.0° .

curve, which is very similar to that in the Rayleigh–Bénard problem, will be referred to as the primary neutral curve. At larger δ , figure 6(a–d) shows a sequence of neutral curves for inclination angles between 65.8° and 68° . At $\delta = 65.8^\circ$, a CDNC appears below the primary neutral curve. This CDNC grows, while the minimum Ra on the primary neutral curve descends as δ increases. These two neutral curves eventually merge smoothly at $\delta = 68^\circ$, as shown in figure 6(d).

One of the features that occurs in the analysis for an inclined slot but which is absent in the vertical case is the existence of a *closed* disconnected neutral curve for the transverse disturbances.

When a CDNC lies entirely below the minimum of the primary neutral curve, three extremal Rayleigh numbers may occur (Pearlstein 1981; Pearlstein *et al.* 1988). The first and second extremal Rayleigh numbers correspond to the minimum and maximum on the CDNC, respectively, while the third extremal Ra corresponds to the minimum on the primary neutral curve. At any Ra between the second and third extremal values, the basic state is stable with respect to all transverse disturbances. However, in this range of Ra , the present flow is unstable with respect to the longitudinal mode, as shown in figure 5. Were this not the case, the basic state would, however, still have been unstable with respect to three-dimensional disturbances. This is because one can find (through the Squire transformation) three-dimensional disturbances with the same total wavenumber $\beta = (\beta_x^2 + \beta_y^2)^{\frac{1}{2}}$ which become unstable at *any* Ra lying above the first extremal value.

We note that there are (isothermal) parallel shear flows (Blennerhassett 1980) in which no longitudinal mode lies below the CDNC. In this case, a successful application of Squire's transformation shows that the flow is sometimes unstable with respect to three-dimensional disturbances of infinitesimal amplitude when it is stable with respect to all two-dimensional ones.

Thus, in the gap between the maximum of the CDNC and the minimum of the primary neutral curve, it is of interest to explore the stability of the flow with respect to *all* sufficiently small two-dimensional disturbances. As the two neutral curves just discussed correspond to the transverse mode, it is only necessary to decide whether longitudinal disturbances can grow in this range of Ra .

The CDNC that appears at $\delta = 66^\circ$ for $Pr = 6.7$ lies above $Ra_{1on}(66^\circ)$, as shown by Hart (1971). Korpela (1974) has computed the crossover angle, δ_{cro} , (below which the transverse mode is critical) as a function of Pr (see his figure 3). Thus, in an effort to find conditions for which Ra_{1on} lies above the maximum of the CDNC, we have decreased Pr until the primary neutral curve and CDNC merge (at $Pr = 1.75$ for $\delta = 65^\circ$, and $Pr = 2.30$ for $\delta = 66^\circ$). In neither case did Ra_{1on} move above the minimum of the CDNC. At $Pr = 1.75$, Ra_{1on} is still smaller than Ra_{tra} , consistent with Korpela's results. For high-Prandtl-number fluids heated from below, the longitudinal mode is critical except when the slot is nearly vertical. For fluids heated from below with $Pr \leq 0.26$, we find that the onset of instability always occurs via the transverse mode. This agrees well with a value of 0.24 reported by Korpela (1974) and is identical to the value reported by Ruth (1980). We have found no region in the (Pr, δ) -space where the CDNC will be physically observable.

Figure 7 shows the stability boundary for $Pr = 0.223$ (mercury), which clearly illustrates that the transverse mode is the critical one for all δ . As discussed by Korpela (1974), Ra_{crit} is no longer a monotonic function of the inclination angle.

It is well known that the number of neutral curves for the Rayleigh-Bénard problem is infinite. To understand how the number of neutral curves changes from one (or from two, when a CDNC accompanies the primary one) to infinity as δ approaches 90° , we let δ increase beyond 68° for $Pr = 6.7$. Figure 8(a-d) shows schematically the neutral curves at various values of δ . The CDNC grows, and after merging with the primary neutral curve, a rightward-pointing 'foot' forms on the new 'combined' neutral curve, as shown in figure 8(a). At $\delta = 84^\circ$, an indentation forms at the lower right. Near $\delta = 87.5^\circ$, a new CDNC appears, which then grows and ultimately merges with the combined neutral curve. At $\delta = 89^\circ$, another (larger) foot

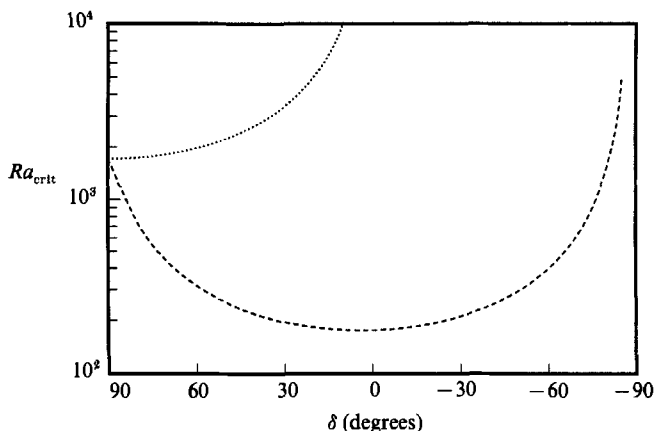


FIGURE 7. Stability boundary for a constant-viscosity fluid with $Pr = 0.223$ (mercury) in an inclined slot. The flow is stable below the transverse mode. $\cdots\cdots$, longitudinal mode; $-----$, transverse mode.

forms. This process is believed to repeat indefinitely between $\delta = 89^\circ$ and 90° , with the indentations and feet moving upwards toward $\beta = 0$ and $\beta = \infty$, respectively. In the limit, an infinite number of neutral curves is formed.

The 'virtual discontinuity' in Ra_{tra} versus Pr reported by Ruth (1980) at $Pr = 2.15$ for free convection in a slot inclined at 25° from the horizontal can be explained by the appearance of the CDNC. In this case, instead of varying δ while keeping Pr fixed, we vary Pr with δ fixed at 65° . For $Pr > 2.15$, there is only one neutral curve, which we again refer to as the primary one. At $Pr = 2.15$, as in the $Pr = 6.7$ case with $\delta = 65.8^\circ$ described above (figure 6a), a CDNC appears below the primary neutral curve. This CDNC grows, while the minimum Ra on the primary neutral curve descends as Pr decreases. At $Pr = 1.75$, these two neutral curves merge smoothly together. It is now clear that the 'virtual discontinuity' at $\delta = 65^\circ$ discussed by Ruth actually corresponds to an S-shaped Ra_{tra} - δ curve between $Pr = 1.75$ and 2.15 in the (Ra_{tra}, Pr) -plane. We have also varied Pr , with δ fixed at 64° , 65° , and 66° . The results are presented as three-dimensional views of neutral surfaces (figure 9a-c) in the (Ra, β, Pr) -space. At $\delta = 64^\circ$, there is only a single neutral curve in the (Ra, β) -plane for all values of Pr . At $\delta = 65^\circ$, a CDNC exists in the range $1.75 < Pr < 2.15$ as discussed above. At $\delta = 66^\circ$, the CDNC exists for all $Pr > 2.30$, below which it merges smoothly into the primary neutral curve. For $Pr > 2.30$, the CDNC decreases in size as Pr increases, but persists and approaches a fixed shape and position in the (Ra, β) -plane as $Pr \rightarrow \infty$.

We note here that the linear stability of the finite-amplitude longitudinal roll solutions for a constant-viscosity free-convection flow in an inclined slot, and the transition to three-dimensional motion, have been considered by Clever & Busse (1977).

5.3. Variable-viscosity fluid in a vertical slot

For a variable-viscosity fluid in a vertical slot, we first consider fluids for which $\mu_e(T) = \mu_0 \exp[-a(T - T_0)]$, previously studied by Thangam & Chen (1986). The dimensionless viscosity-temperature relation can be written as

$$f_e(\theta) = \frac{\mu_e(T_0 + \theta \Delta T)}{\mu_0} = \exp[-a(\Delta T)\theta] = \exp(-c\theta). \quad (5.1)$$

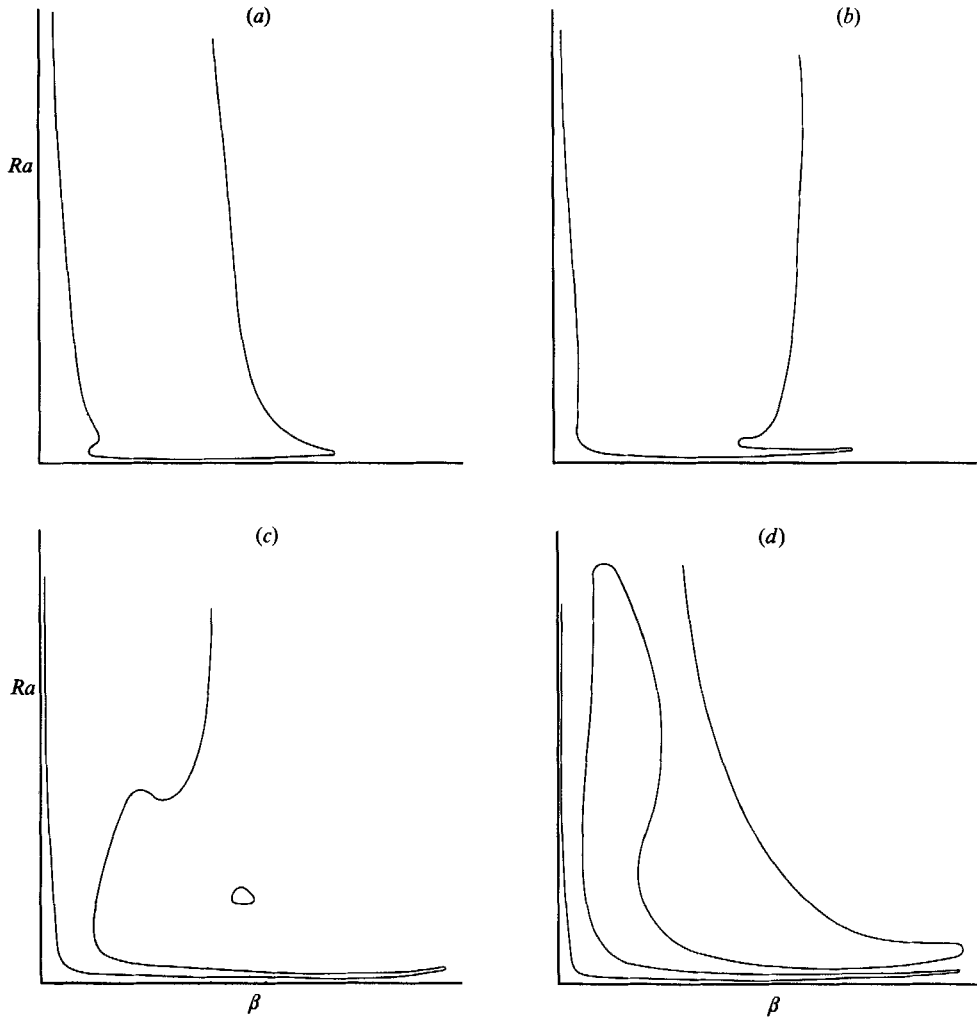


FIGURE 8. Neutral curve(s) for a constant-viscosity fluid with $Pr = 6.7$ in an inclined slot, shown schematically for graphical clarity. (a) $\delta = 80.0^\circ$, (b) 84.0° , (c) 87.5° , (d) 89.0° . The sequence of CDNC growth and merging is believed to repeat indefinitely in $89^\circ < \delta < 90^\circ$, leading to an infinity of neutral curves for $\delta = 90^\circ$.

The viscosity contrast is then e^c . Figure 10 shows the critical Grashof number ($Gr_{\text{crit}} = Ra_{\text{crit}}/Pr$) as a function of Pr for various values of c . As discussed above for the constant-viscosity case, there is a $Pr^{\text{tr}} (\approx 12.5)$ above which the onset of secondary flow occurs via oscillatory disturbances. Also, a jump occurs in the critical wavenumber, β_{crit} , at Pr^{tr} . For the variable-viscosity case, however, both neutral curves are oscillatory. This is because the basic velocity profile is no longer symmetric about the midplane; a wave speed is now associated with the hydrodynamic mode, as discussed by Thangam & Chen (1986). At Pr^{tr} a mode change accompanied by a jump in β_{crit} occurs in the variable-viscosity case also, as shown in figure 11. For each c considered, the critical Grashof number remains almost constant for $Pr < Pr^{\text{tr}}$, which indicates that the instability mechanism is a hydrodynamic one. For $Pr > Pr^{\text{tr}}$, Gr_{crit} decreases with Pr . At a much higher Prandtl number, we find another jump in the critical wavenumber for $c = 1$ and $c = 3$, but

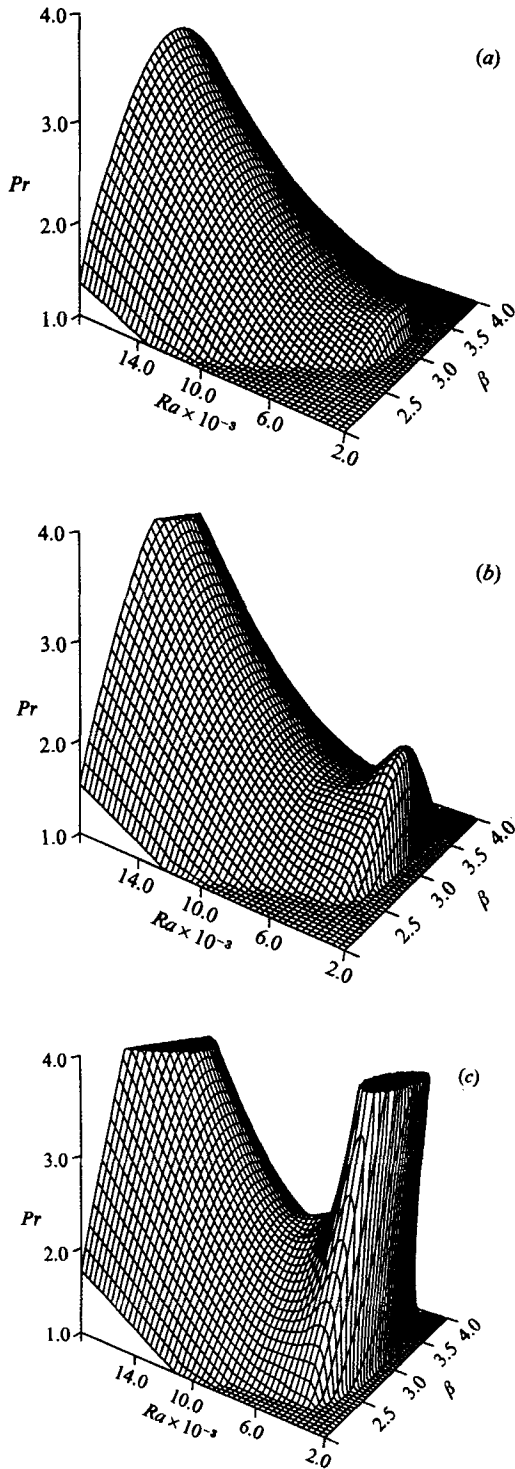


FIGURE 9. Neutral surface in (Ra, β, Pr) -space for a constant-viscosity fluid in an inclined slot. (a) $\delta = 64^\circ$, (b) 65° , (c) 66° . Note the disconnectedness of the Ra - β neutral curves for sufficiently large Pr at $\delta = 65^\circ$ and 66° . (The flat surface in the $Pr = 1$ plane is not part of the neutral surface and has been included for graphical clarity only.)

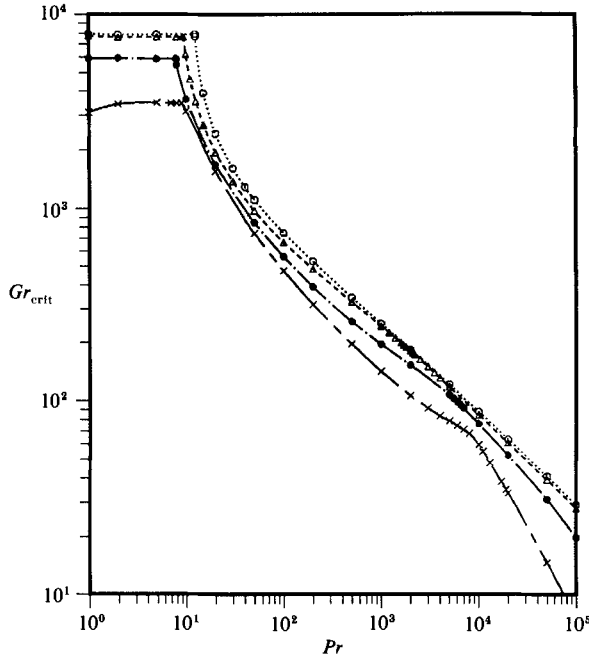


FIGURE 10. Variation of Gr_{crit} with Pr for $f(\theta) = \exp(-c\theta)$ in a vertical slot. $\circ \cdots \circ$, $c = 0$; $\triangle \cdots \triangle$, $c = 1$; $\bullet \cdots \bullet$, $c = 3$; $\times \cdots \times$, $c = 5$ (\circ , \triangle , \bullet , \times indicate computed (Pr, Gr_{crit}) pairs). Note the similarity of the $Gr_{crit}-Pr$ curves over the central three decades of Pr .

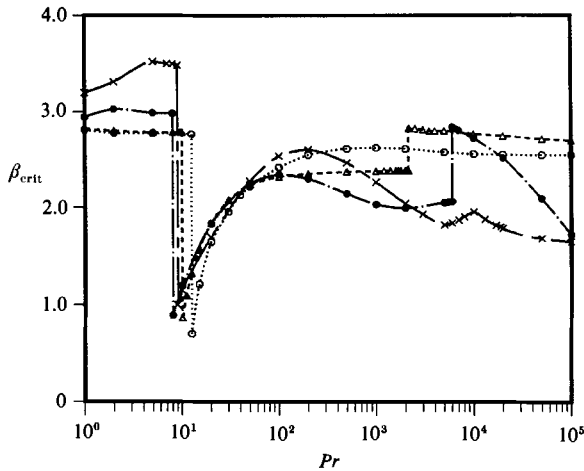


FIGURE 11. Variation of β_{crit} with Pr for $f(\theta) = \exp(-c\theta)$ in a vertical slot. $\circ \cdots \circ$, $c = 0$; $\triangle \cdots \triangle$, $c = 1$; $\bullet \cdots \bullet$, $c = 3$; $\times \cdots \times$, $c = 5$ (\circ , \triangle , \bullet , \times indicate computed (Pr, β_{crit}) pairs). Note the discontinuous change in β_{crit} near $Pr = 10$ for each value of c shown.

not for $c = 5$ or for the constant-viscosity fluid. For $c = 1$, figure 12 shows a second transition in the critical wavenumber, similar to that displayed in figure 3(a). As in figure 3(c), the intersection of two oscillatory neutral-curve branches is not a bifurcation point.

Contrary to the assertion of Thangam & Chen (1966) that variable-viscosity effects

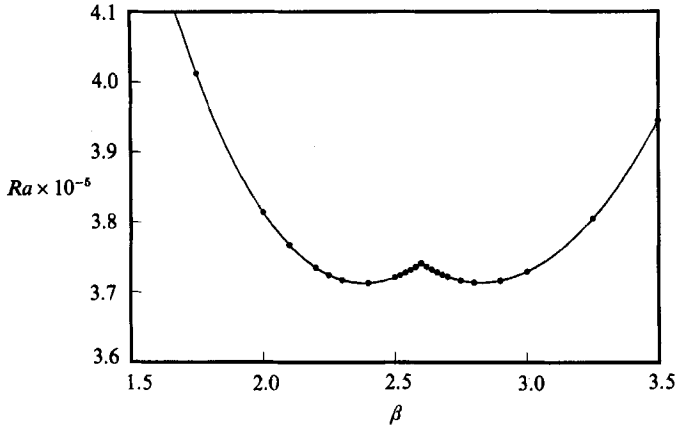


FIGURE 12. Neutral curves for $f(\theta) = \exp(-\theta)$ with $Pr = 2100$ in a vertical slot. The existence of two local minima on the oscillatory neutral curve is accompanied by a discontinuous change in β_{crit} .

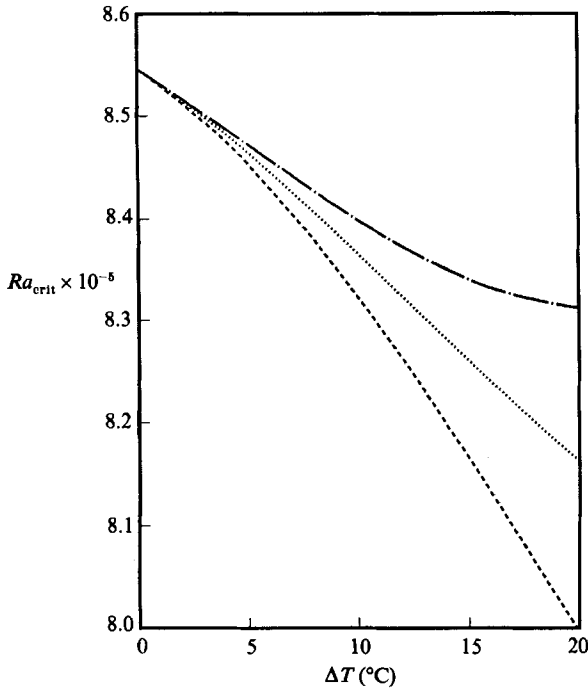


FIGURE 13. Ra_{crit} as a function of ΔT for 99% aqueous glycerol in a vertical slot. -----, exponential form; ·····, Arrhenius form; —·—·—·—, four-parameter fit.

are negligible for $Pr \leq 100$, we find that for all Pr , the onset of instability in a fluid with an exponential $\mu(T)$ occurs at values of Ra_{crit} considerably less than those predicted using constant μ . As the viscosity contrast increases for fixed Pr , the basic state becomes unstable at a lower value of Gr_{crit} , as figure 10 clearly shows.

To assess the importance of $\mu(T)$ in determining the stability of parallel free-convection flow in a vertical slot, we have determined Ra_{crit} for three approximations to the actual $\mu(T)$ for 99% glycerol as a function of ΔT across the layer. The results, shown in figure 13, indicate that the exponential and Arrhenius forms give good

agreement with the predictions using the actual $\mu(T)$. The maximum variation shown (for $\Delta T = 20^\circ$) corresponds to a relative error in Ra_{crit} of about 4%. A noteworthy feature is that for the vertical slot the relative error associated with the Arrhenius form is only about one-half that of the exponential form. This is to be contrasted to the onset of motion in a horizontal aqueous glycerol (99%) layer heated from below (Chen & Pearlstein 1988), in which the Arrhenius and actual forms of $\mu(T)$ gave virtually indistinguishable values of Ra_{crit} , with the exponential form giving results differing by about the same amount (3%) as in the vertical-slot case.

Clearly, the dependence of Gr_{crit} on the viscosity contrast is not nearly so great as might be supposed on the basis of the work on boundary layers (Wazzan, Okamura & Smith 1968; Strazisar, Reshotko & Prah 1977). At low Pr , the values of Re_{crit} obtained for $c = 0$ and $c = 3$ (corresponding to constant viscosity and a viscosity contrast of about 20, respectively) in the present case differ by only about 25%. As pointed out by Thangam & Chen, the instability mechanism at low Pr is identical to that for an isothermal parallel base flow with the given velocity profile, previously studied by Birikh (1966). We note that these profiles are inflexional and lose their stability via an essentially inviscid mechanism. Thus, it is not surprising that at low Pr the present instability is less sensitive to both the details of the basic velocity profile, and the interaction of the disturbances with the viscosity stratification, than is the Tollmien-Schlichting mechanism. At higher Pr , the inviscid mechanism is modified by coupling to the energy balance, and competes with the buoyancy-driven instability discussed in §5.1.

5.4. Variable-viscosity fluid in an inclined slot

The Ra_{crit} versus δ plots discussed in §5.2 (figures 5 and 7) show that the stability boundary can have two different topologies in the constant-viscosity case. At high Pr (e.g. figure 5), the stability boundary consists of two branches: one corresponding to the longitudinal mode for $\delta_{\text{cro}} \leq \delta \leq 90^\circ$; and the other to the transverse mode for $-90^\circ < \delta < \delta_{\text{cro}}$. At sufficiently low Pr (figure 7), the stability boundary corresponds entirely to the transverse mode. As discussed by Korpela (1974), the transition occurs at $Pr = 0.24$, in such a way that for $Pr \leq 0.24$, Ra_{tra} initially decreases as δ decreases from 90° and after passing through a minimum before reaching $\delta = 0$, increases monotonically thereafter.

For a variable-viscosity fluid, however, the stability boundary can be somewhat more complicated, as shown in figure 14(a-e) for a fluid with $Pr = 2$ having an exponential dependence of μ on T , with different values of the viscosity contrast e^c . For $c = 1$, figure 14(a) shows results that are virtually identical to the constant-viscosity case for $Pr = 2$, and are topologically similar to those for $Pr = 6.7$ (figure 5). For $c = 3$ (figure 14b), Ra_{tra} has developed a local minimum to the left of δ_{cro} . Thus, Ra_{crit} is still a monotonic function of δ . For $c = 5$ (figure 14c), the local minimum of Ra_{tra} occurs near δ_{cro} , which has itself increased. For larger values of c , the local minimum moves to the right of δ_{cro} , and occurs on the transverse portion of the stability boundary (figure 14d for $c = 7$). Thus, Ra_{crit} is no longer a monotonic function of δ . Ultimately, the local maximum on the Ra_{tra} curve disappears (figure 14e for $c = 14$) and the stability boundary consists only of a transverse branch. The latter situation is topologically similar to that found by Korpela (1974) in a constant-viscosity fluid for $Pr \leq 0.24$. We note that, for a horizontal layer with $\mu(T) = \mu_e(T)$, Stengel *et al.* (1982) have shown that Ra_{crit} is a unimodal function of c , achieving its maximum value at $c = 8$. Thus, for $c = 14$, the $\delta = 90^\circ$ intercept of Ra_{lon} is a decreasing function of c .

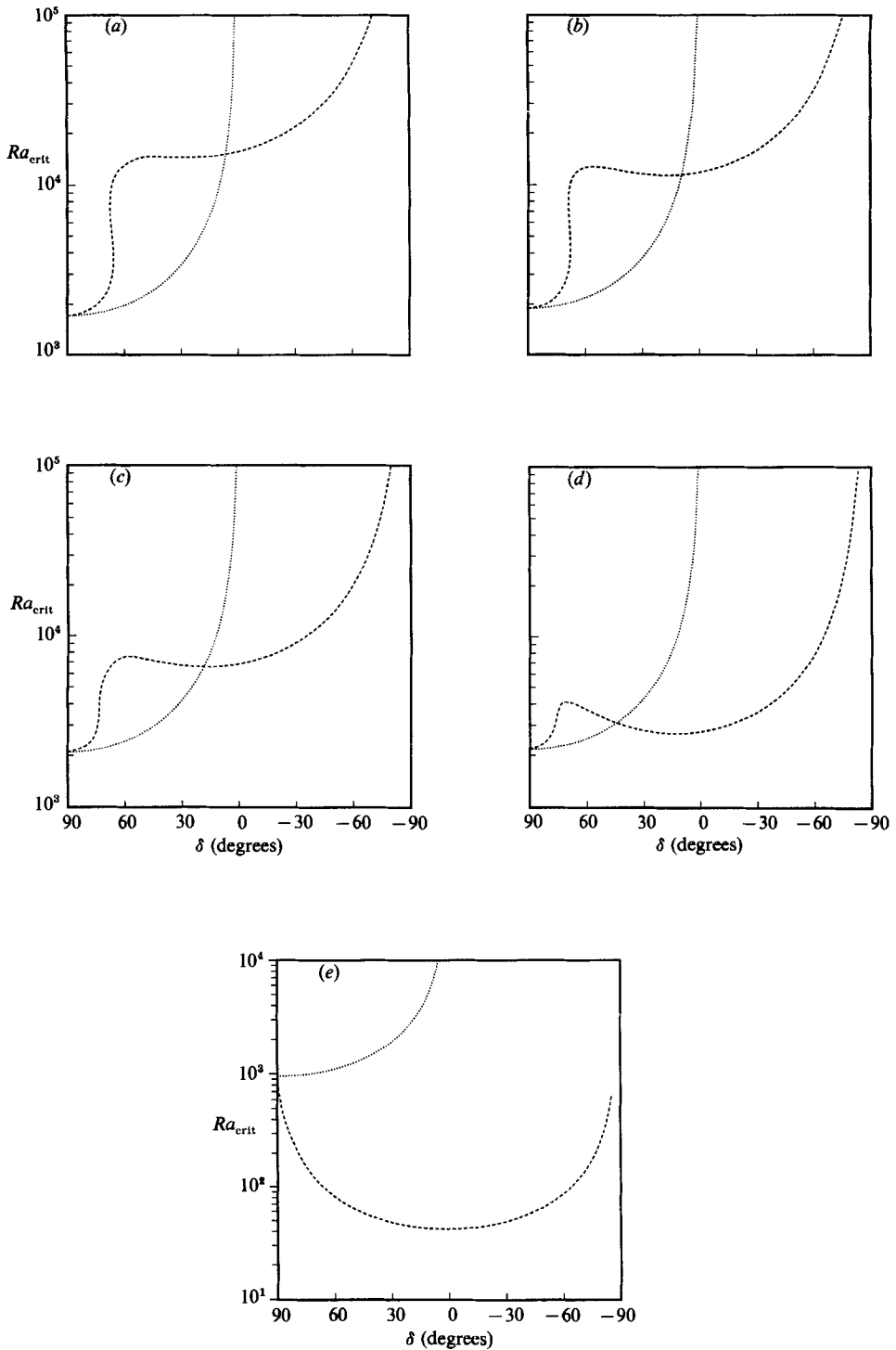


FIGURE 14. Stability boundaries for $f(\theta) = \exp(-c\theta)$ with $Pr = 2$ in an inclined slot. (a) $c = 1$, (b) 3, (c) 5, (d) 7, (e) 14. \cdots , longitudinal mode; $---$, transverse mode. Note the appearance of a local minimum on the $Ra_{tra}-\delta$ curve, which at larger c leads to the loss of monotonicity by the $Ra_{crit}-\delta$ stability boundary.

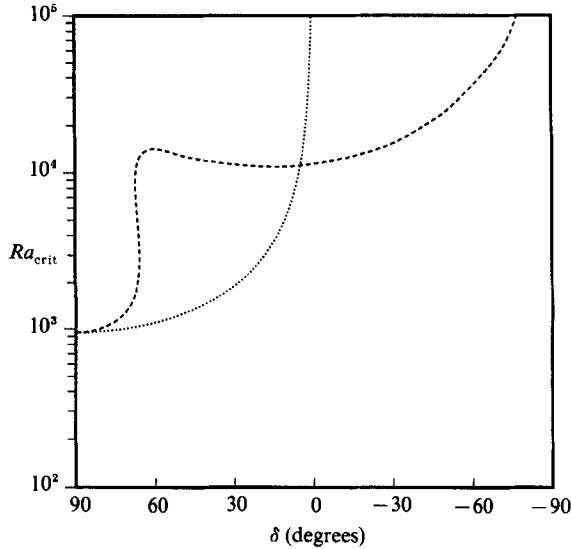


FIGURE 15. Stability boundary for $f(\theta) = \exp(-14\theta)$ with $Pr = 500$ in an inclined slot. \cdots , longitudinal mode; $---$, transverse mode. For this high- Pr case, note the change in the critical mode near $\delta = 0^\circ$.

Figure 15 shows that for larger Pr , Ra_{tra} does not become unimodal, even at very large viscosity contrasts. For $Pr = 500$ and $c = 14$, the stability boundary consists of a (Pr -independent) longitudinal branch over almost the entire range of positive δ , and a transverse branch that is critical for $-90^\circ < \delta < \delta_{cro}$.

For a fluid with $Pr = 2$ and $\mu(T) = \mu_e(T)$, figure 16 shows Ra_{tra} as a function of δ for four values of c . We note that as c increases from zero, Ra_{tra} develops a local maximum in the vicinity of $\delta = 66^\circ$, where the existence of a CDNC renders Ra_{tra} multivalued for small c . As c increases, the local maximum occurs at larger values of δ (closer to the horizontal), and smaller values of Ra . The multivaluedness is lost between $c = 1$ and $c = 3$. For $Pr = 2$ and $1 \leq c \leq 7$, figure 16 also shows that, as c increases, the transverse mode is destabilized for $-90^\circ \leq \delta \leq 62^\circ$ and stabilized for $72^\circ \leq \delta \leq 90^\circ$. In the intervening range of δ , Ra_{tra} is a non-monotonic function of c . The effect of increasing c on Ra_{tra} at 90° is consistent with the results of Stengel *et al.* (1982) discussed above.

The viscosity-temperature dependence of many liquids and geophysical materials is very well approximated by the Arrhenius form (Iyer 1930; Fowler 1985). Thus, we have investigated the error which will occur in using the exponential approximation to $\mu_A(T)$. As discussed in Chen & Pearlstein (1988), two parameters (which we take to be the viscosity contrast and dimensionless temperature difference) are required to characterize the dependence of Ra_{crit} on $\mu_A(T)$. Figure 17 shows, for $\Delta T/T_0 = 0.1$ (corresponding to $\Delta T = 30^\circ$ at room temperature) and a viscosity contrast of e^7 , that values of Ra_{crit} predicted by $\mu_e(T)$ are consistently below those predicted by $\mu_A(T)$.† The relative error, a non-increasing function of δ , is about 5% (independent of δ) for the longitudinal mode, and decreases from about 17% to 9% for the transverse mode as δ increases from -85° to δ_{cro} . This difference in the relative errors is consistent

† One might also use a least-squares fit of $\mu_e(T)$ to this $\mu_A(T)$. This gave a viscosity contrast of $\exp(6.992)$, which was judged to be insufficiently different from the $\mu_e(T)$ used to justify a separate stability calculation.

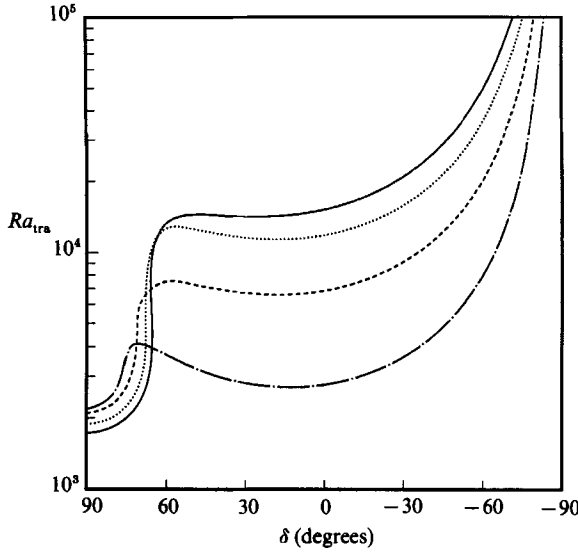


FIGURE 16. Ra_{tra} versus δ for $f(\theta) = \exp(-c\theta)$ with $Pr = 2$ in an inclined slot. —, $c = 1$; \cdots , $c = 3$; $-\cdots-$, $c = 5$; $-\cdot-\cdot-$, $c = 7$. Note the non-monotonic nature of the Ra_{tra} - δ curve for $c \geq 3$.

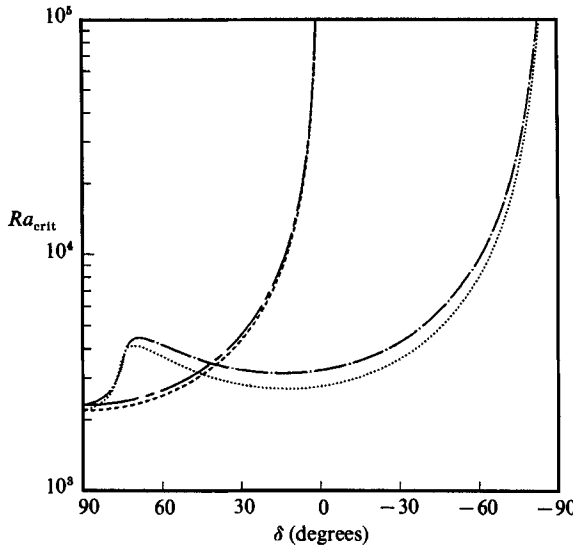


FIGURE 17. Stability boundaries for a fluid with viscosity contrast of e^7 , $\Delta T/T_0 = 0.1$, $Pr = 2$. $-\cdots-$, exponential form, longitudinal mode; \cdots , exponential form, transverse mode; $-\cdot-\cdot-$, Arrhenius form, longitudinal mode; $-\cdots-$, Arrhenius form, transverse mode. Note that the relative difference between the predictions using the Arrhenius and exponential forms is considerably small for the longitudinal mode than for the transverse mode.

with the fact that the longitudinal instability is buoyancy-driven, while the transverse mode arises from an instability of the parallel shear flow set up by the buoyancy force. One expects, and figure 17 confirms, that the buoyancy-driven instability is less sensitive to the details of the viscosity stratification.

We have computed the stability boundaries (Ra_{crit} vs. δ) for aqueous glycerol

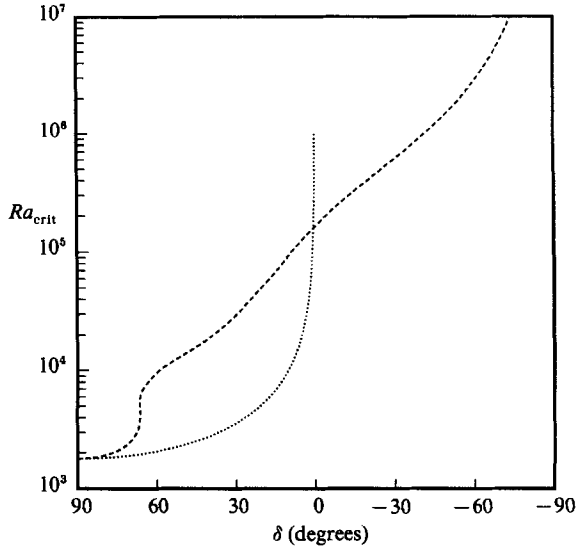


FIGURE 18. Stability boundary for aqueous glycerol ($\gamma = 0.8$) in an inclined slot. $\cdots\cdots$, longitudinal mode; $-----$, transverse mode.

solutions with $\gamma = 0.8, 0.9$, and 0.99 in an inclined slot. In figure 18, we present results for $\gamma = 0.8$ and $\Delta T = 20^\circ\text{C}$; results for other values of γ and ΔT are very similar. For a wide range of ΔT , the stability boundary consists of two parts. For the transverse mode, a CDNC still exists near $\delta = 66^\circ$. When the flow is heated from below, the longitudinal mode becomes unstable at an Ra_{crit} that lies below the minimum of the transverse neutral curve over virtually the entire range of positive δ . As shown in figure 3 of Korpela (1974), the crossover from the transverse to the longitudinal mode occurs at $\delta = 1^\circ$ for $Pr = 12$. From that figure, and from figure 15 for a high-Prandtl-number fluid with large viscosity contrast, one may also infer that for Pr on the order of 500 or more, δ_{cro} is less than 1° . Thus, for a high-Prandtl-number fluid in an inclined slot heated from below, one can predict, by means of a suitable rescaling (cf. (3.1)), the onset of instability simply from the results for the horizontal case with the same $f(\theta)$, previously considered by Stengel *et al.* (1982), and Chen & Pearlstein (1988). (See the latter for further references.) In the range $-90^\circ < \delta < \delta_{\text{cro}}$, the transverse mode is the only possible source of instability.

For sufficiently high Pr , instability sets in via the transverse mode only when the slot is nearly vertical, or when the layer is heated from above. In the former case, the results are very similar to those for the vertical slot. It is only when the layer is heated from above that one needs to perform the linear stability analysis for a high-Prandtl-number fluid in an inclined slot. We find that for a given glycerol-water solution heated from above with δ fixed, Ra_{crit} decreases as ΔT (i.e. viscosity contrast) increases. At constant ΔT , Ra_{crit} increases as the glycerol concentration increases.

6. Relationship to previous experimental work

Given the existence of significant discrepancies in the literature between theory and experiment (Chen & Thangam 1985), between various theoretical predictions (Brenier *et al.* 1986; Gershuni & Zhukhovitskii 1976; Korpela *et al.* 1973; Thangam & Chen 1986), and the discontinuous variation of Ra_{tra} with Pr reported by Ruth

	Remarks	Glycerol mass fraction, γ		
		0.7	0.8	0.9
T_0^{expt} (°C)	Chen & Thangam	21.5	22.7	33.4
$\Delta T_{\text{crit}}^{\text{expt}}$ (°C)	Chen & Thangam	17.4	31.9	49.1
$\Delta T_{\text{crit}}^{\text{nh}}$ (°C)	Present work, computed using T_0^{expt}	4.0	13.8	28.7
$Ra_{\text{crit}}^{\text{expt}} \times 10^{-5}$	Chen & Thangam, corresponds to $\Delta T_{\text{crit}}^{\text{expt}}$	4.10	3.42	3.32
$Ra_{\text{crit}}^{\text{th},1} \times 10^{-5}$	Chen & Thangam, computed using $\Delta T_{\text{crit}}^{\text{expt}}$	1.51	1.71	1.40
$Ra_{\text{crit}}^{\text{th},2} \times 10^{-5}$	Present work, corresponds to $\Delta T_{\text{crit}}^{\text{nh}}$	0.94	1.48	1.94
$Ra_{\text{crit}}^{\text{th},3} \times 10^{-5}$	Present work, computed using $\Delta T_{\text{crit}}^{\text{expt}}$	0.88	1.36	1.67
$\beta_{\text{crit}}^{\text{expt}}$	Chen & Thangam	3.1	2.9	3.4
$\beta_{\text{crit}}^{\text{th},1}$	Chen & Thangam, computed using $\Delta T_{\text{crit}}^{\text{expt}}$	2.39	2.46	2.24
$\beta_{\text{crit}}^{\text{th},2}$	Present work, computed using $\Delta T_{\text{crit}}^{\text{nh}}$	2.48	2.40	2.26
$\beta_{\text{crit}}^{\text{th},3}$	Present work, computed using $\Delta T_{\text{crit}}^{\text{expt}}$	2.36	2.21	2.06

TABLE 1. Comparison of theoretical and experimental values of ΔT_{crit} , Ra_{crit} , and β_{crit}

(1980), we devoted considerable effort to analysing these special cases with our computer code. On the basis of the excellent agreement between our results for the special cases of a constant-viscosity fluid in vertical (Korpela *et al.* 1973, cf. §5.1), inclined (Hart 1971; Korpela 1974, cf. §5.2), and horizontal (Stengel *et al.* 1982, cf. Chen & Pearlstein 1988) variable-viscosity fluid layers, we believe that our code is correct and that our results are accurate.

One of the questions outstanding from the work of Chen & Thangam (1985) on the stability of the free-convection flow of a variable-viscosity fluid in a vertical slot concerns the differences between their measured and computed values of Ra_{crit} . The experimental values of Ra_{crit} were approximately twice the theoretical values (computed by their linear stability analysis).

We have used the four-parameter fit (Chen & Pearlstein 1987) to the $\mu(T)$ behaviour of concentrated aqueous glycerol solutions to compute the critical Rayleigh numbers and wavenumbers in the experiments of Chen & Thangam (1985). Our results are shown in table 1. In a variable-viscosity fluid, ΔT and Ra are *not* linearly related. We have fixed T_0 at its experimental value and computed Ra_{crit} in two different ways. One method is to use ΔT_{crit} (from Chen & Thangam's experiment) to obtain the minimum and maximum temperatures in the viscosity relation, and to then compute Ra_{crit} using that f . The other method involves iterating on ΔT (with Ra computed from its definition in terms of the physical properties and plate separation d), until this Ra lies at the minimum of the neutral curve.

In general, one can see that our values of Ra_{crit} and β_{crit} , while differing substantially from the theoretical predictions of Chen & Thangam, do not exhibit significantly better agreement with their experiments. Thus, the disagreement between theory and experiment in Chen & Thangam (1985) cannot be completely attributed to an error in their analysis, which is probably responsible for the differences between their value of Pr^{eff} (Thangam & Chen 1986) and those computed by Korpela *et al.* (1973), Brenier *et al.* (1986), and in the present work (cf. §5.1). Neither can the disagreement be attributed to subcritical instability, as the experimental values of Ra_{crit} exceed those predicted by the linear stability analysis.

In an effort to better understand the nature of the discrepancy, we have computed the stream function corresponding to the neutral eigenfunction of the linear stability

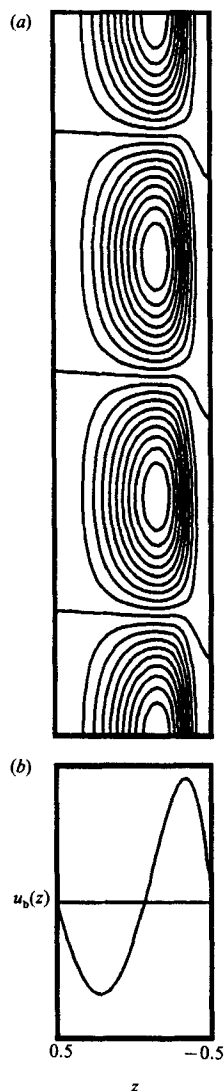


FIGURE 19. Disturbance stream function (a) and base-velocity profile (b) for a 90% glycerol-water solution in a vertical slot. $\Delta T = 49.1$ °C, $T_0 = 33.4$ °C, and $d = 2$ cm. Note that the disturbance is concentrated near the hot wall.

problem at β_{crit} for the conditions pertaining to the 90% glycerol experiment of Chen & Thangam. The results are shown in figure 19(a). Figure 19(b) shows the computed parallel base-velocity profile for the same conditions. In agreement with the experimental results of Chen & Thangam, the disturbance is localized in a region considerably narrower than the channel. Moreover, the ratio of the thicknesses of the relatively undisturbed portions of the flow adjacent to the hot and cold walls appears to be in excellent agreement with the flow visualizations of Chen & Thangam.

These results bear on the suggestion of Chen & Thangam (1985) that the localized secondary flow arises as an instability of a base flow having a 'nearly motionless' central core region. As discussed by them and Elder (1965), this type of base flow occurs in vertical slots of finite aspect ratio at sufficiently high Ra . This is consistent

with the results of Gill & Davey (1969) and Gill & Kirkham (1970) who showed that for $Pr = O(1000)$, the aspect ratio of 15 used by Chen & Thangam is not large enough for the results to be independent of the box length. Our results show that the confinement of the disturbance to the central core does *not* depend on the deviation of the basic velocity and temperature distributions from their fully developed forms.

We also remark that the shadowgraph flow-visualization technique employed by Chen & Thangam may also be responsible for the apparent discrepancy between theory and experiment. As pointed out by Elder, 'These cells are very weak, and near the critical Rayleigh number are extremely difficult to detect, especially when the wavelength is large'. The difficulty is exacerbated by the fact that, in a cell of finite aspect ratio, onset typically occurs via a breakup of the large unicellular motion into two cells of widely disparate sizes, with the larger of the two occupying almost the entire length of the slot (Elder 1965). This greatly complicates the detection of onset.

Finally, Seki *et al.* (1978) conducted an extensive set of experiments in a vertical slot of variable aspect ratio using glycerol and a high-Prandtl-number transformer oil. We have not undertaken any comparison to their results for several reasons. First, the work of Seki *et al.* was not directed to establishing conditions for the onset of secondary flow. No experimental determination of the stability boundary was attempted. Thus, at best one can only determine whether an experimentally unstable base flow should be stable or unstable according to linear analysis. More importantly, even though $\mu(T)$ is available for the transformer oil (H. Inaba, private communication 1986), the temperature differences ΔT and the average temperatures T_0 are not. Thus, with only the Rayleigh numbers reported by Seki *et al.*, the variation of μ across the slot is unknown, and we are thus unable to compute even the basic state.

The authors thank Professor A. G. Lavine for her careful reading of the manuscript. This work was supported in part by Unocal, and by funds provided under the matching provisions of the NSF Presidential Young Investigator Award Program. The authors gratefully acknowledge the provision of computing services at the San Diego Supercomputer center under the auspices of the NSF Office of Advanced Scientific Computing.

REFERENCES

- BATCHELOR, G. K. 1954 Heat transfer by free convection across a closed cavity between vertical boundaries at different temperatures. *Q. Appl. Maths* **12**, 209–233.
- BERGHOLZ, R. F. 1978 Instability of steady natural convection in a vertical fluid layer. *J. Fluid Mech.* **84**, 743–768.
- BIRIKH, R. V. 1966 On small perturbations of a plane parallel flow with cubic velocity profile. *Prikl. Mat. Mekh.* **30**, 356–361 (*Appl. Math. Mech.* **30**, 432–438).
- BIRIKH, R. V., GERSHUNI, G. Z., ZHUKHOVITSKII, E. M. & RUDAKOV, R. N. 1968 Hydrodynamic and thermal instability of a steady convective flow. *Prikl. Mat. Mekh.* **32**, 256–263 (*Appl. Math. Mech.* **32**, 246–252).
- BIRIKH, R. V., GERSHUNI, G. Z., ZHUKHOVITSKII, E. M. & RUDAKOV, R. N. 1972 On oscillatory instability of plane-parallel convective motion in a vertical channel. *Prikl. Mat. Mekh.* **36**, 745–748 (*Appl. Math. Mech.* **36**, 707–710).
- BLENNERHASSETT, P. J. 1980 On the generation of waves by wind. *Phil. Trans. R. Soc. Lond.* **A 298**, 451–494.

- BRENIER, B., ROUX, B. & BONTOUX, P. 1986 Comparaison des méthodes Tau-Chebyshev et Galerkin dans l'étude de stabilité des mouvements de convection naturelle. Problème des valeurs propres parasites. *J. Méc. Théor. Appl.* **5**, 95-119.
- CAREY, V. P. & MOLLENDORF, J. C. 1978 Natural convection in liquids with temperature dependent viscosity. In *Proc. 6th Intl Heat Transfer Conf.*, Vol. 2, pp. 211-216. Hemisphere.
- CATTON, I. 1978 Natural convection in enclosures. In *Proc. 6th Intl Heat Transfer Conf.*, Vol. 6, pp. 13-31. Hemisphere.
- CHANDRASEKHAR, S. 1961 *Hydrodynamic and Hydromagnetic Stability*. Clarendon.
- CHEN, C. F. & THANGAM, S. 1985 Convective stability of a variable-viscosity fluid in a vertical slot. *J. Fluid Mech.* **161**, 161-173.
- CHEN, Y.-M. & PEARLSTEIN, A. J. 1987 Viscosity-temperature correlation for glycerol-water solutions. *Ind. Engng Chem. Res.* **26**, 1670-1672.
- CHEN, Y.-M. & PEARLSTEIN, A. J. 1988 Onset of convection in variable viscosity fluids: assessment of approximate viscosity-temperature relations. *Phys. Fluids* **31**, 1380-1385.
- CLEVER, R. M. & BUSSE, F. H. 1977 Instabilities of longitudinal convection rolls in an inclined layer. *J. Fluid Mech.* **81**, 107-127.
- DENN, M. M. 1975 *Stability of Reaction and Transport Processes*, p. 146. Prentice Hall.
- DI PAOLA, G. & BELLEAU, B. 1975 Apparent molal volumes and heat capacities of some tetraalkylammonium bromides, alkyltrimethylammonium bromides, and alkali halides in aqueous glycerol solutions. *Can. J. Chem.* **53**, 3452-3461.
- ELDER, J. W. 1965 Laminar free convection in a vertical slot. *J. Fluid Mech.* **23**, 77-98.
- FINLAYSON, B. A. 1972 *The Method of Weighted Residuals and Variational Principles*. Academic Press.
- FOWLER, A. C. 1985 A simple model of convection in the terrestrial planets. *Geophys. Astrophys. Fluid Dyn.* **31**, 283-309.
- GAGE, K. S. & REID, W. H. 1968 The stability of thermally stratified plane Poiseuille flow. *J. Fluid Mech.* **33**, 21-32.
- GALLAGHER, A. P. 1969 On a proof by Petrov of the stability of plane Couette flow and plane Poiseuille flow. *SIAM J. Appl. Maths* **17**, 765-768.
- GARROW, B. S., BOYLE, J. M., DONGARRA, J. J. & MOLER, C. B. 1977 *Matrix Eigensystem Routines - EISPACK Guide Extension*. Springer.
- GERSHUNI, G. Z. 1953 On the stability of plane convective motion of a fluid. *Zh. Tekh. Fiz.* **23**, 1838-1844.
- GERSHUNI, G. Z. 1955 On the problem of stability of a plane convective fluid flow. *Zh. Tekh. Fiz.* **25**, 351-357.
- GERSHUNI, G. Z. & ZHUKHOVITSKII, E. M. 1969 Stability of plane-parallel convective motion with respect to spatial perturbations. *Prikl. Mat. Mekh.* **33**, 855-860 (*Appl. Math. Mech.* **33**, 830-835).
- GERSHUNI, G. Z. & ZHUKHOVITSKII, E. M. 1976 *Convective Stability of Incompressible Fluids*. Jerusalem: Keter.
- GILL, A. E. & DAVEY, A. 1969 Instabilities of a buoyancy-driven system. *J. Fluid Mech.* **35**, 775-798.
- GILL, A. E. & KIRKHAM, C. C. 1970 A note on the stability of convection in a vertical slot. *J. Fluid Mech.* **42**, 125-127.
- GOLDSTEIN, R. J. & WANG, Q.-J. 1984 An interferometric study of the natural convection in an inclined water layer. *Intl J. Heat Mass Transfer* **27**, 1445-1453.
- HART, J. E. 1971 Stability of the flow in a differentially heated inclined box. *J. Fluid Mech.* **47**, 547-576.
- HOLLANDS, K. G. T. & KONICEK, L. 1973 Experimental study of the stability of differentially heated inclined air layers. *Intl J. Heat Mass Transfer* **16**, 1467-1476.
- HOOGENDOORN, C. J. 1986 Natural convection in enclosures. In *Proc. 8th Intl Heat Transfer Conf.*, Vol. 1, 111-120. Hemisphere.
- IYER, M. P. V. 1930 The temperature variation of the viscosity of liquids and its theoretical significance. *Indian J. Phys.* **5**, 371-383.

- KORPELA, S. A. 1974 A study on the effect of Prandtl number on the stability of the conduction regime of natural convection in an inclined slot. *Intl J. Heat Mass Transfer* **17**, 215–222.
- KORPELA, S. A., GÖZÜM, D. & BAXI, C. B. 1973 On the stability of the conduction regime of natural convection in a vertical slot. *Intl J. Heat Mass Transfer* **16**, 1683–1690.
- KURZWEIG, U. H. 1970 Stability of natural convection within an inclined channel. *Trans. ASME C: J. Heat Transfer* **92**, 190–191.
- LITOVITZ, T. A. 1952 Temperature dependence of the viscosity of associated liquids. *J. Chem. Phys.* **20**, 1088–1089.
- OSTRACH, S. 1982 Natural convection heat transfer in cavities and cells. In *Proc. 7th Intl Heat Transfer Conf.*, Vol. 1, pp. 365–379. Hemisphere.
- PEARLSTEIN, A. J. 1981 Effect of rotation on the stability of a doubly diffusive fluid layer. *J. Fluid Mech.* **103**, 389–412.
- PEARLSTEIN, A. J., HARRIS, R. M. & TERRONES, G. 1988 The onset of convective instability in a triply diffusive fluid layer. *J. Fluid Mech.* (submitted).
- RAITHBY, G. D. & HOLLANDS, K. G. T. 1985 Natural convection. In *Handbook of Heat Transfer Fundamentals*, 2nd edn (ed. W. M. Rohsenow, J. P. Hartnett & E. N. Ganic), chap. 6. McGraw-Hill.
- RUDAKOV, R. N. 1966 On small perturbations of convective motion between vertical parallel planes. *Prikl. Mat. Mekh.* **30**, 362–368 (*Appl. Math. & Mech.* **30**, 439–445).
- RUDAKOV, R. N. 1967 Spectrum of perturbations and stability of convective motion between vertical planes. *Prikl. Mat. Mekh.* **31**, 349–355 (*Appl. Math. & Mech.* **31**, 376–383).
- RUTH, D. W. 1979 On the transition to transverse rolls in an infinite vertical fluid layer – a power series solution. *Intl J. Heat Mass Transfer* **22**, 1199–1208.
- RUTH, D. W. 1980 On the transition to transverse rolls in inclined infinite fluid layers – steady solutions. *Intl J. Heat Mass Transfer* **23**, 733–737.
- RUTH, D. W., HOLLANDS, K. G. T. & RAITHBY, G. D. 1980 On free convection experiments in inclined air layers heated from below. *J. Fluid Mech.* **96**, 461–479.
- SEGUR, J. B. 1953 Physical properties of glycerol and its solutions. In *Glycerol* (ed. C. S. Miner & N. N. Dalton), pp. 238–334. Reinhold.
- SEGUR, J. B. & OBERSTAR, H. E. 1951 Viscosity of glycerol and its aqueous solutions. *Ind. Engng Chem.* **43**, 2117–2120.
- SEKI, N., FUKUSAKO, S. & INABA, H. 1978 Visual observation of natural convective flow in a narrow vertical cavity. *J. Fluid Mech.* **84**, 695–704.
- SHAABAN, A. H. & ÖZISIK, M. N. 1983 The effect of nonlinear density stratification on the stability of a vertical water layer in the conduction regime. *Trans. ASME C: J. Heat Transfer* **105**, 130–137.
- SMITH, M. K. 1988 Thermal convection during the directional solidification of a pure liquid with variable viscosity. *J. Fluid Mech.* **188**, 547–570.
- STENGEL, K. C., OLIVER, D. S. & BOOKER, J. R. 1982 Onset of convection in a variable-viscosity fluid. *J. Fluid Mech.* **120**, 411–431.
- STRAZISAR, A. J., RESHOTKO, E. & PRAHL, J. M. 1977 Experimental study of the stability of heated laminar boundary layers in water. *J. Fluid Mech.* **83**, 225–247.
- THANGAM, S. & CHEN, C. F. 1986 Stability analysis on the convection of a variable viscosity fluid in an infinite vertical slot. *Phys. Fluids* **29**, 1367–1372.
- TOULOUKIAN, Y. S. & MAKITA, T. 1970 *Thermophysical Properties of Matter*. The TPRC Data Series, Vol. 6. IFI/Plenum.
- VEDHANAYAGAM, M., LIENHARD, J. H. & EICHORN, R. 1979 Method for visualizing high Prandtl number heat convection. *Trans. ASME C: J. Heat Transfer* **101**, 571–573.
- VEST, C. M. & ARPACI, V. S. 1969 Stability of natural convection in a vertical slot. *J. Fluid Mech.* **36**, 1–15.
- WAZZAN, A. R., OKAMURA, T. & SMITH, A. M. O. 1968 The stability of water flow over heated and cooled flat plates. *Trans. ASME C: J. Heat Transfer* **90**, 109–114.
- WEAST, R. C., ASTLE, M. J. & BEYER, W. H. 1986 *CRC Handbook of Chemistry and Physics*. CRC Press.